Autophagy 9:4, 496–509; April 2013; © 2013 Landes Bioscience

Visualizing the autophagy pathway in avian cells and its application to studying infectious bronchitis virus

Helena J. Maier,[1] Eleanor M. Cottam,[2] Phoebe Stevenson-Leggett,[1] Jessica A. Wilkinson,[1] Christopher J. Harte,[1] Tom Wileman[2] and Paul Britton[1,*]

[1]The Pirbright Institute; Compton Laboratory; Compton, Newbury, Berkshire UK; [2]Biomedical Research Centre; Norwich Medical School; Faculty of Medicine and Health; University of East Anglia; Norwich, UK

Keywords: GFP-LC3, LC3A, LC3B, LC3C, autophagy, avian, chicken, coronavirus, infectious bronchitis virus, primary cells, recombinant adenovirus

Abbreviations: (E)GFP, (enhanced) green fluorescent protein; MAP1LC3/LC3, microtubule-associated protein 1 light chain 3; CK, chick kidney; CEF, chick embryo fibroblast; IBV, infectious bronchitis virus; Nsp, nonstructural protein; MOI, multiplicity of infection; MHV, mouse hepatitis virus; SARS-CoV, severe acute respiratory syndrome coronavirus; DMV, double-membrane vesicle; Ad5, human adenovirus type 5; rAd, recombinant adenovirus; CsCl, cesium chloride; PBS, phosphate-buffered saline; LAMP1, lysosomal-associated membrane protein 1; DAPI, 4',6-diamidino-2-phenylindole; SPF, specified pathogen free; CPE, cytopathic effect; FM, full-nutrient media; FCS, fetal calf serum; HBSS, Hank's balanced salt solution; WM, wortmannin

Autophagy is a highly conserved cellular response to starvation that leads to the degradation of organelles and long-lived proteins in lysosomes and is important for cellular homeostasis, tissue development and as a defense against aggregated proteins, damaged organelles and infectious agents. Although autophagy has been studied in many animal species, reagents to study autophagy in avian systems are lacking. Microtubule-associated protein 1 light chain 3 (MAP1LC3/LC3) is an important marker for autophagy and is used to follow autophagosome formation. Here we report the cloning of avian LC3 paralogs A, B and C from the domestic chicken, *Gallus gallus domesticus*, and the production of replication-deficient, recombinant adenovirus vectors expressing these avian LC3s tagged with EGFP and FLAG-mCherry. An additional recombinant adenovirus expressing EGFP-tagged LC3B containing a G120A mutation was also generated. These vectors can be used as tools to visualize autophagosome formation and fusion with endosomes/lysosomes in avian cells and provide a valuable resource for studying autophagy in avian cells. We have used them to study autophagy during replication of infectious bronchitis virus (IBV). IBV induced autophagic signaling in mammalian Vero cells but not primary avian chick kidney cells or the avian DF1 cell line. Furthermore, induction or inhibition of autophagy did not affect IBV replication, suggesting that classical autophagy may not be important for virus replication. However, expression of IBV nonstructural protein 6 alone did induce autophagic signaling in avian cells, as seen previously in mammalian cells. This may suggest that IBV can inhibit or control autophagy in avian cells, although IBV did not appear to inhibit autophagy induced by starvation or rapamycin treatment.

Introduction

Autophagy plays a critical role in many cellular processes, including the degradation of misfolded protein aggregates, clearance of microorganisms and sustaining cells during starvation, as well as during development and aging (reviewed in refs. 1–5). The use of green fluorescent protein (GFP)-tagged ATG8 in yeast[6,7] or the mammalian ortholog, microtubule-associated protein 1 light chain 3 (MAP1LC3, henceforth LC3)[8,9] has become indispensable for visualizing the formation of autophagosomes and tracking autophagy in cells. Furthermore, a recombinant adenovirus expressing mammalian GFP-LC3B has been used to study autophagy in primary rat hepatocytes.[10] To date, the process of autophagy in avian systems has been little studied and few reagents are available. GFP-tagged avian ATG5 has been used to study aging in chicken cells.[11] However, ATG5 only labels the phagophore and dissociates from the membrane upon formation of the complete autophagosome.[12] Conversely, GFP-LC3 remains associated with the autophagosome membrane and can be used to study formation of autophagosomes through to fusion with endosomes and lysosomes.[8,12,13] To aid the study of autophagy in avian systems, including primary cells, recombinant adenoviruses expressing EGFP- and FLAG-mCherry- tagged versions of the three avian LC3 paralogs, LC3 A, B and C, were generated.

*Correspondence to: Paul Britton; Email: paul.britton@pirbright.ac.uk
Submitted: 06/27/12; Revised: 12/19/12; Accepted: 01/02/13
http://dx.doi.org/10.4161/auto.23465

All three avian genes were cloned to allow comparison of the role of the three expressed proteins in autophagy. In addition, a recombinant adenovirus expressing EGFP-tagged LC3B containing a G120A mutation was constructed as a genetic control for the inhibition of autophagy.

Construction of these tools is not only useful for studying autophagy in an avian system but also for studying the role of autophagy in economically important viral diseases. Autophagy has been implicated in clearance of intracellular pathogens but it has also been shown that viruses are able to use the pathway to benefit their own replication (reviewed in refs. 14-16). Inhibition of autophagy results in increased replication of Sindbis virus,[17] herpes simplex virus 1 (HSV-1)[18] and vesicular stomatitis virus (VSV)[19] and HSV-1 and γ-herpesviruses encode mechanisms to evade autophagy.[18,20,21] Conversely, viruses also use autophagy to increase their replication. Influenza A virus induces autophagy and evidence exists that autophagosome accumulation supports Influenza A virus replication,[22] but most studies find no alteration in infectious viral titer production upon inhibition of autophagy.[23-25] HIV-1 Gag protein induces autophagy and associates with LC3, possibly to aid Gag processing, while Nef prevents fusion of the autophagosome with the lysosome and subsequent degradation of the virus.[26] Furthermore, several viruses including dengue virus and poliovirus utilize the membrane structures generated during autophagy as a platform for the assembly of viral replication complexes.[27,28] During coronavirus infection, double-membrane vesicles, that resemble autophagosomes, are generated, potentially providing a platform for viral RNA synthesis.[29,30] Furthermore, the coronavirus mouse hepatitis virus (MHV) has been shown previously to induce autophagy in infected cells,[31] although whether a complete autophagy pathway is required for efficient virus replication remains unclear.[31-33] Recent work has demonstrated that the avian coronavirus, infectious bronchitis virus (IBV), induces autophagy in mammalian cells.[34] Furthermore, expression of nonstructural protein 6 (Nsp6) alone from IBV, as well as Nsp6 homologs from related coronaviruses and arteriviruses, is able to induce autophagy.[34]

Here we report further investigation into the role of autophagy in the replication cycle of IBV. We demonstrated using the new reagents generated in this study, that although IBV induced autophagic signaling in Vero cells, no such induction occurred following infection of avian cells. Furthermore, this was not dependent upon virus pathogenicity and virus replication was unaffected by induction or inhibition of autophagy. Interestingly, expression of Nsp6 alone did induce autophagic signaling in avian cells, suggesting that IBV may have developed a strategy to inhibit or control autophagy upon infection. Despite this, IBV was not able to inhibit autophagy induction by starvation or rapamycin treatment.

Results

Identification of avian LC3 orthologs. Due to the wide use of GFP-tagged mammalian LC3B as a marker for autophagy in mammalian cells,[8-10] we decided to produce avian LC3 proteins tagged with EGFP and FLAG-mCherry to investigate autophagy in avian cells. Furthermore, initial work utilizing several commercially available antibodies against human LC3 showed that these antibodies did not cross-react or detect chicken LC3 in our specific cell of interest, primary CK cells, by immunofluorescence. A bioinformatic search of the chicken Ensembl database identified sequences predicted to be the avian *LC3A*, *LC3B* and *LC3C* ortholog genes within the genome of the Red Junglefowl (*Gallus gallus*). These sequences were compared with *LC3A*, *LC3B* and *LC3C* genes identified in other species (**Fig. 1**). The comparisons showed that the avian *LC3* orthologs were highly related to counterparts in other species and sequence identity was supported by conserved gene synteny for all three avian genes. Furthermore, the identified avian genes clustered together with their orthologous genes from other species in a phylogenetic tree (**Fig. 1D**). Therefore chicken *LC3A*, *LC3B* and *LC3C* sequences were RT-PCR-amplified (**Table 1**) from mRNA derived from primary CK cells isolated from SPF Rhode Island Red chicks and recombinant adenoviruses expressing the three EGFP-Av-LC3 and FLAG-mCherry-Av-LC3 paralogs, as well as EGFP-Av-LC3B containing a G120A mutation, were generated, as described in *Materials and Methods*. Sequence analysis confirmed that the amino acid sequences of the chicken-derived LC3A, LC3B and LC3C EGFP-tagged sequences within the recombinant adenoviruses were identical to those of the Red Junglefowl.

Avian EGFP-LC3 paralogs respond to treatments to induce or inhibit autophagy. The utility of the three avian EGFP-LC3 paralogs expressed from the recombinant adenovirus vectors in studying autophagic signaling was investigated initially in primary CK cells. Cells were transduced with either a control adenovirus expressing GFP, rAd5-GFP (kindly provided by Sharon Tooze[10]) or rAd5-EGFP-Av-LC3A, -LC3B or -LC3C. Twenty-four hours post-transduction, cells were incubated for 2 h under conditions known to induce or inhibit autophagy. Transduced control cells incubated in full-nutrient medium (FM) were compared with transduced cells incubated in either HBSS, to induce autophagy, or in HBSS with 10 nM wortmannin, a PI3 kinase/PtdIns 3-kinase inhibitor known to inhibit autophagosome formation. Confocal microscopy analysis revealed that GFP, expressed from rAd5-GFP, had a diffuse distribution throughout the cytoplasm and the nucleus of the CK cells and that distribution was unaffected by any of the treatments (**Fig. 2A**). Similarly, when CK cells were transduced with rAd5-EGFP-Av-LC3A or -LC3B and incubated in full-nutrient media the EGFP-Av-LC3 signal was observed to be distributed diffusely throughout the cytoplasm and the nucleus (**Fig. 2A**). When CK cells were transduced with rAd-EGFP-Av-LC3C and incubated in full-nutrient media, the EGFP-Av-LC3C distribution was observed to be diffuse in the cytoplasm and the nucleus, but there was also some reticular localization (**Fig. 2A**). However, when the CK cells were starved in HBSS, EGFP-Av-LC3A, -LC3B and -LC3C proteins were relocated to distinct cytoplasmic puncta, suggestive of autophagosome formation (**Fig. 2A**). As can be observed from **Figure 2A**, the puncta associated with autophagosome formation did not form in starved cells in the presence of wortmannin, showing that, as seen for autophagy induction in other animal systems, formation of EGFP-LC3 puncta was dependent on class

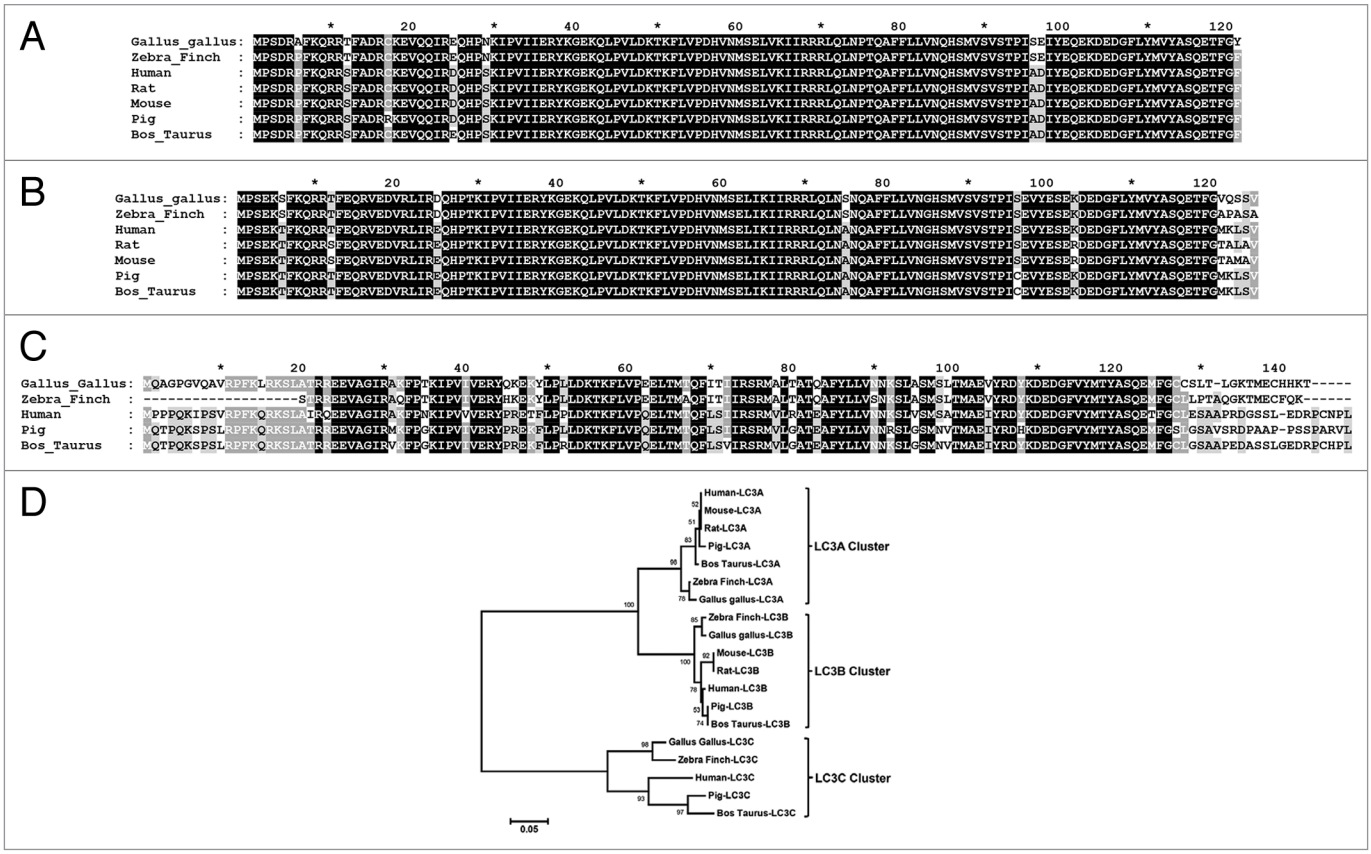

Figure 1. Comparison of the LC3A, LC3B and LC3C protein amino acid sequences derived from different species. The individual amino acid sequences of the (**A**) LC3A, (**B**) LC3B and (**C**) LC3C proteins were identified in the NCBI database, aligned using ClustalX version 2.1[35] and compared using GeneDoc Multiple Sequence Alignment Editor and Shading Utility version 2.7.001 (www.nrbsc.org/gfx/genedoc/). The LC3A protein accession numbers used were Gallus gallus XP_417327.2, Zebra Finch NP_001232518.1, Human NP_115903.1, Mouse NP_080011.1, Rat NP_955794.1, Pig NP_001164298.1, Bos taurus NP_001039640.1. The LC3B protein accession numbers used were Gallus gallus NP_001026632.1, Zebra Finch NP_001232222.1, Human NP_073729.1, Mouse NP_080436.1, Rat NP_074058.2, Pig NP_001177219.1, Bos taurus NP_001001169.1. The LC3C protein accession numbers used were Gallus gallus XP_419549.2, Human NP_001094528.1, Pig XP_003130606.1, Bos taurus NP_001094528.1 and Zebra Finch database ID TR:H0ZK62_TAEGU. (**D**) Phylogenetic analysis of the three LC3 paralogs following clustalX alignment of all the LC3 protein sequences. Phylogenetic analysis was conducted using MEGA4 version 4[36] in which the clustalX alignment was analyzed by the neighbor joining method using a bootstrap of 500 replications and a random seed of 64238.

III PtdIns3K activity. Finally, as shown in **Figure 2B**, for EGFP-Av-LC3A, EGFP-Av-LC3B and EGFP-Av-LC3C there was a significant increase in the number of puncta per cell in CK cells starved in HBSS when compared with those incubated in FM and that this increase in puncta number was inhibited in the presence of wortmannin. There was no change in the number of puncta per cell in CK cells expressing GFP from rAd5-GFP.

To confirm these observations, experiments were repeated in other widely used avian cell types, primary CEFs (**Fig. 2C**) and the avian continuous cell line, DF1 (**Fig. 2D**). As observed in CK cells, expression of all three EGFP-tagged avian LC3 paralogs resulted in a significant increase in the number of puncta per cell in HBSS starved cells and that this increase in puncta formation was inhibited in the presence of wortmannin in both CEFs and DF1 cells. These results demonstrated that the three EGFP-tagged avian LC3 paralogs expressed from recombinant adenovirus can be used to visualize autophagic signaling in either an avian cell line or in primary avian cells.

Figure 2 (See opposite page). EGFP-Av-LC3 paralogs are markers for autophagy in primary chick kidney (CK) cells, chick embryo fibroblasts (CEFs) and DF1 cells. (**A**) CK cells were transduced with rAd-EGFP-Av-LC3A, rAd-EGFP-Av-LC3B, rAd-EGFP-Av-LC3C or rAd-GFP. After 24 h cells were washed and incubated in full media (FM; control), Hank's balanced salt solution (HBSS; to induce autophagy) or HBSS containing 10 nM wortmannin (HBSS+WM; to inhibit HBSS-induced autophagy). Nuclei (blue) were stained with DAPI. Scale bars, 10 μm. (**B**) Number of puncta per cell was determined from (**A**) using Imaris spots software. (**C**) CEF cells were treated as in (**A**) and puncta per cell determined as in (**B**). (**D**) DF1 cells were treated as in (**A**) and puncta per cell determined as in (**B**). Open bars, FM treated cells; closed bars, HBSS treated cells; hashed bars, HBSS+WM treated cells. (**E**) CK cells were transduced with rAd-EGFP-Av-LC3B or rAd-EGFP-Av-LC3B G120A. After 24 h cells were washed and incubated in HBSS. Nuclei were stained with DAPI. Scale bars: 10 μm. (**F**) Number of puncta per cell was determined from (**E**) using Imaris spots software. Mean plus standard deviation is shown for at least 20 cells counted from three independent experiments. **$p \leq 0.01$ in a Student's t-test. (**G**) DF1 cells were transduced with rAd-EGFP, rAd-EGFP-Av-LC3B or rAd-EGFP-Av-LC3B G120A. After 24 h cells were washed and incubated for 1 h in FM, HBSS or HBSS continaing 10 nM wortmannin. Cells were lysed and lysates run on 10% NuPAGE in MOPS buffer. Western blots were performed with anti-GFP or anti-actin.

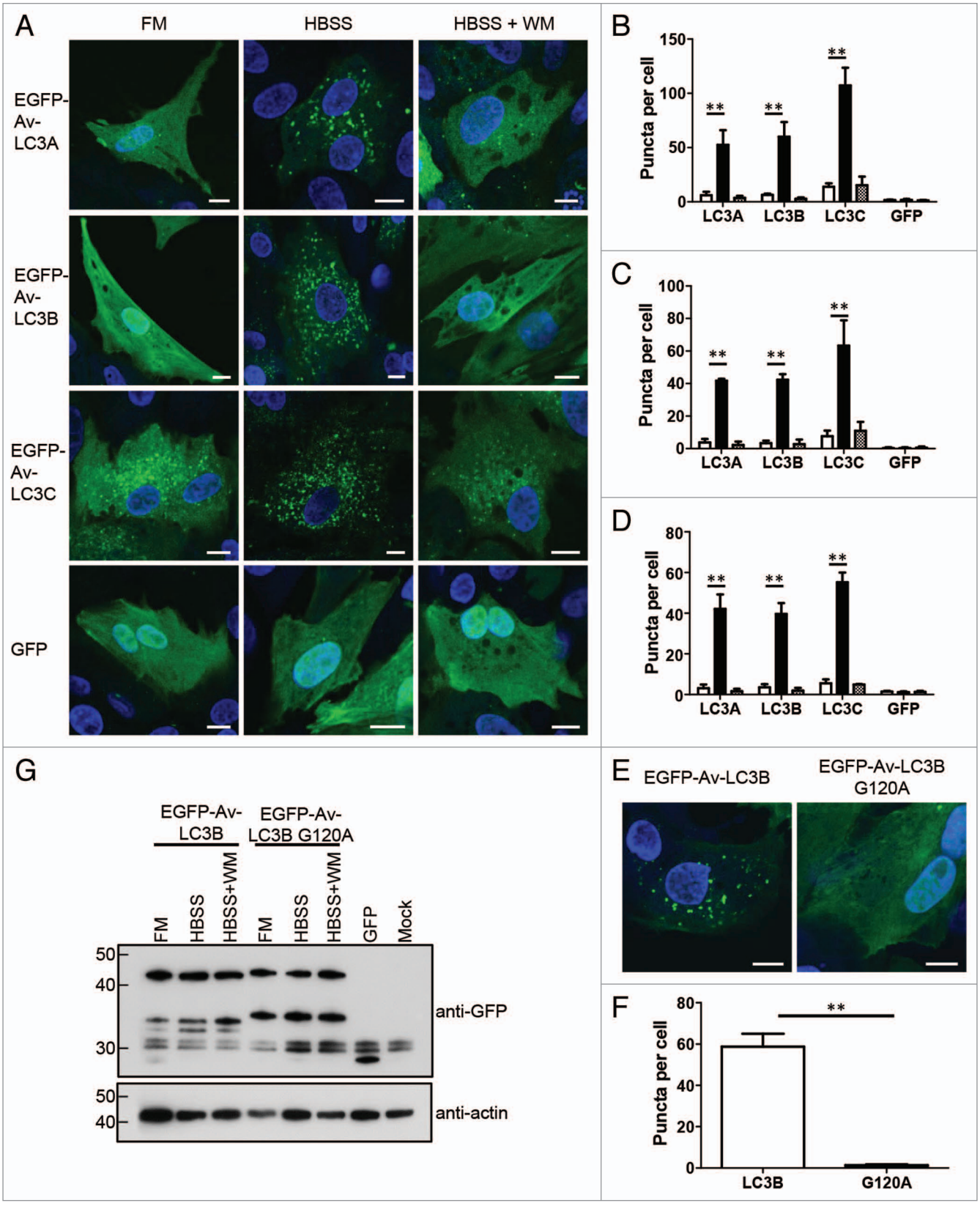

Figure 2. For figure legend, see page 498.

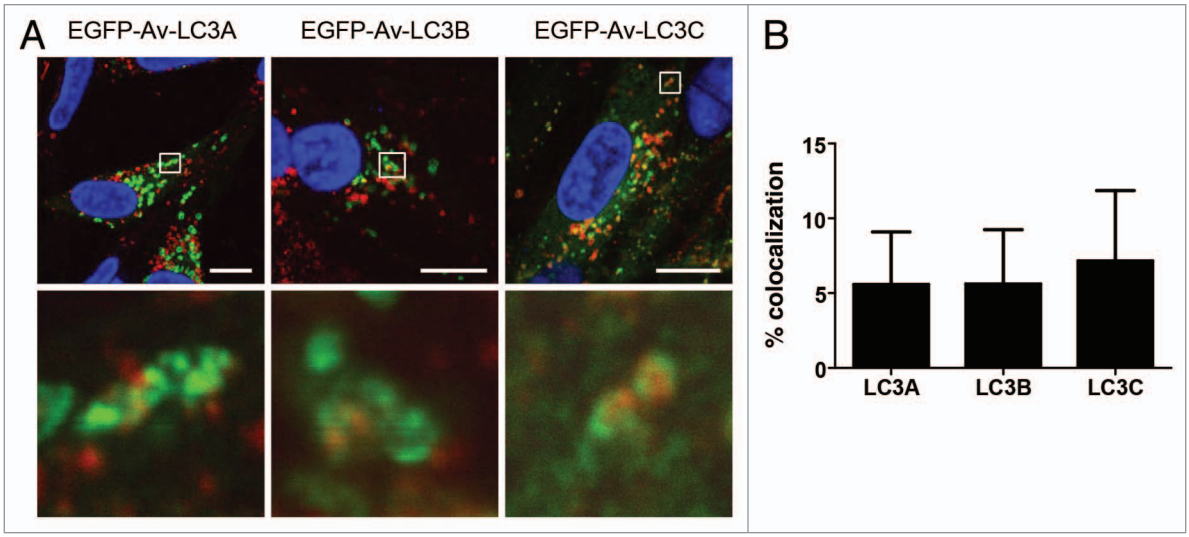

Figure 3. EGFP-Av-LC3-labeled autophagosomes fuse with endosomes/lysosomes. (**A**) CEFs were transduced with a recombinant adenovirus expressing avian EGFP-LC3A, -LC3B or -LC3C. After 24 h, cells were incubated in Hank's balanced salt solution for 2 h to induce autophagy. Endosomes/lysosomes were labeled using anti-LAMP1 (red). Regions of colocalization (boxed) are enlarged below each image. Nuclei (blue) were stained with DAPI. Scale bars: 10 μm. (**B**) The percent EGFP signal colocalized with LAMP1 was quantified from (**A**) using Imaris coloc module. Mean plus standard deviation is shown from three independent experiments.

Further experiments were performed to confirm that LC3 puncta observed were as a result of post-translational cleavage of LC3 at position G120 and lipidation, giving rise to LC3-II. CK cells were transduced with a recombinant adenovirus expressing EGFP-tagged avian LC3B G120A or a wild-type control and were starved in HBSS to induce autophagy. **Figure 2E and F** show that while starvation of cells expressing wild-type EGFP-Av-LC3B induced puncta, significantly fewer puncta were observed in cells expressing EGFP-Av-LC3B G120A. In addition, to confirm that avian LC3 is lipidated following induction of autophagic signaling to give LC3-II, DF1 cells were transduced with recombinant adenovirus expressing GFP, EGFP-Av-LC3B or EGFP-Av-LC3B G120A. After 24 h, cells were washed and incubated for an additional hour in full-nutrient media, HBSS or HBSS containing 10 nM wortmannin. Cells were lysed and analyzed by NuPAGE (Invitrogen) followed by western blotting. In all lanes, two nonspecific background bands were detected at 32 and 33 kDa (**Fig. 2G**). In cells expressing EGFP-LC3B or EGFP-LC3B G120A, EGFP-LC3-I was detected at the predicted molecular mass of 42 kDa, with the G120A mutant migrating at a slightly higher molecular mass due to the inhibition of cleavage at G120. In addition, a second EGFP-LC3 associated band was detected at 36 kDa, presumably with a deletion at the N terminus in EGFP because migration at a slightly higher molecular mass was still observed for the G120A mutant. Finally, the EGFP-LC3-II band was detected at 35 kDa. Upon starvation of cells expressing EGFP-Av-LC3B in HBSS, there was an increase in the level of LC3-II compared with cells incubated in full-nutrient media. This increase in level was not seen in the presence of wortmannin. As expected, in cells expressing EGFP-Av-LC3B G120A, the LC3-II band could not be detected.

Autophagosomes labeled with avian EGFP-LC3 paralogs fuse with endosomes/lysosomes. The final steps in the autophagy pathway are the fusion of autophagosomes with endosomes to form amphisomes and with lysosomes to form autolysosomes. Therefore, these final crucial steps in the autophagy pathway were studied in avian cells in which the autophagosomes were labeled with the three EGFP-tagged avian LC3 paralogs. Primary CEF cells were transduced with the recombinant adenoviruses as before and 24 h later the cells were transferred into HBSS for 2 h to induce autophagy and allow incorporation of the EGFP-tagged LC3 paralogs into autophagosomes. Endosomes and lysosomes were visualized by labeling with anti-LAMP1.[37] Observation of the CEF cells transduced with rAd5-EGFP-Av-LC3A, -LC3B or -LC3C and incubated in HBSS to activate autophagy demonstrated a degree of colocalization of the punctate EGFP-Av-LC3A, -LC3B and -LC3C-labeled autophagosomes with endosomes/lysosomes (**Fig. 3A**). The colocalization of EGFP-LC3 with LAMP1 was quantified as 5.6% for both EGFP-Av-LC3A and -LC3B and 7.2% for EGFP-Av-LC3C (**Fig. 3B**). Although the percent of colocalized signal is low, Pearson's correlation coefficients of above 0.5 indicate positive colocalization (**Table 2**). This observation indicates that autophagosomes containing EGFP-Av-LC3A, -LC3B or -LC3C fuse with endosomes/lysosomes, allowing the progression of the full autophagy pathway to be visualized in avian cells, using these reagents.

Avian EGFP- and FLAG-mCherry- LC3 paralogs partially colocalize upon induction of autophagic signaling. The use of mammalian LC3B as a marker protein for autophagy has been well studied. However, the role of LC3A and LC3C in autophagy is less well defined. To determine whether the three different paralogs of avian LC3 localize to the same structures upon autophagy induction, primary CK cells were transduced with both EGFP- and FLAG-mCherry tagged versions of the three avian LC3 paralogs. After 24 h, cells were starved for 2 h in HBSS to

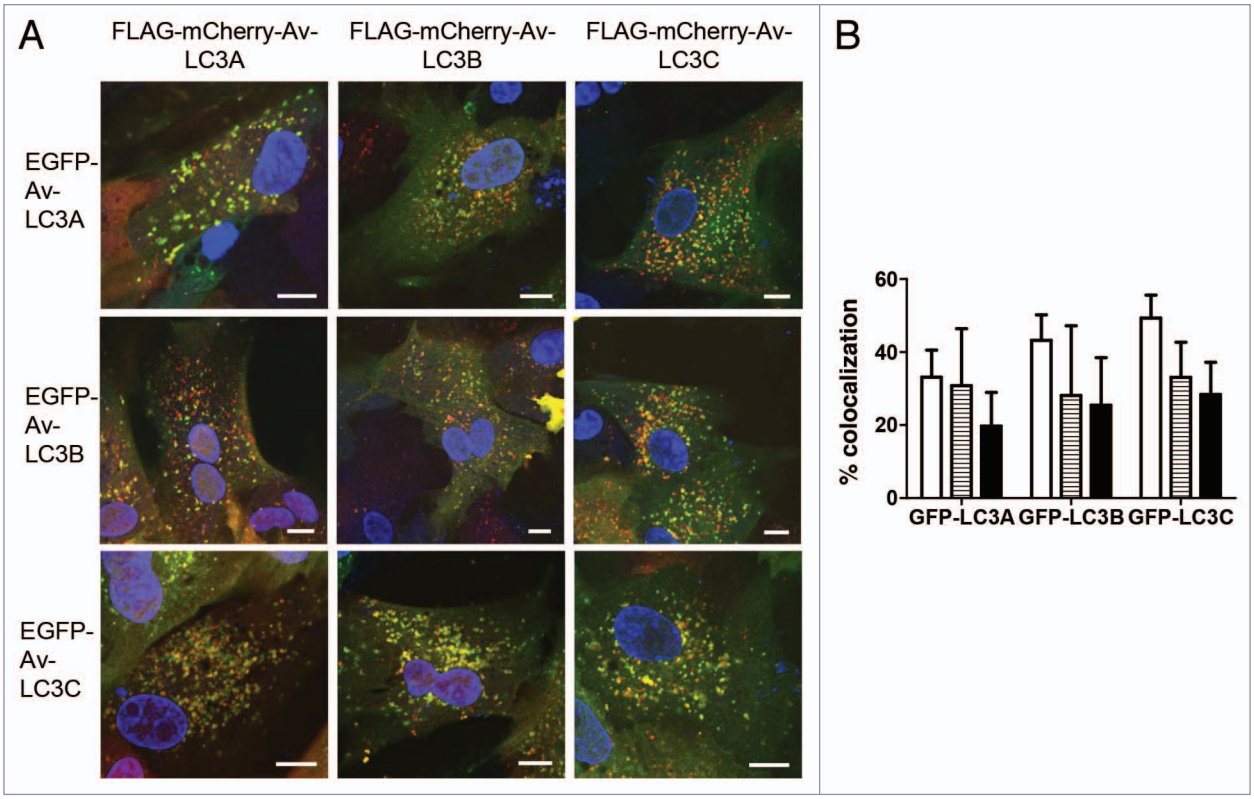

Figure 4. All LC3 paralogs partially colocalize upon induction of autophagic signaling. (**A**) CK cells were transduced with recombinant adenoviruses encoding both EGFP- and FLAG-mCherry-tagged LC3 paralogs. After 24 h cells were starved for 2 h in HBSS to induce autophagic signaling. Nuclei (blue) were stained with DAPI. Scale bars: 10 μm. (**B**) The percent EGFP signal colocalized with mCherry signal was quantified from (**A**) using Imaris coloc module. Open bars, FLAG-mCherry-LC3A; hashed bars, FLAG-mCherry-LC3B; closed bars, FLAG-mCherry-LC3C. Mean plus standard deviation is shown from three independent experiments.

induce autophagic signaling and the location of the two paralogs was determined by confocal fluorescence microscopy. As can be seen from **Figure 4**, all combinations of the paralogs partially colocalized upon induction of autophagy, with colocalization of EGFP signal with mCherry signal varying from 19.7% to 49.3% with Pearson's correlation coefficients of above 0.5 indicating positive colocalization (**Table 3**). This suggests that all three paralogs of avian LC3 associate with autophagosomes and act as marker proteins.

Infectious bronchitis virus induces autophagic signaling in Vero cells but not in avian cells. Previous work has demonstrated that IBV infection of Vero cells induces autophagy, using endogenous LC3B as a marker.[34] Furthermore, expression of the replicase nonstructural protein 6 (Nsp6) alone induced autophagy via an omegasome intermediate.[34] We wanted to determine whether IBV infection could induce autophagic signaling in avian cells. As rat-derived GFP-LC3B is commonly used in studies of autophagy function and the role of autophagy in virus replication,[8,10,28,34,38-40] subsequent experiments using IBV were performed using avian LC3B. Primary CK cells and DF1 cells were transduced with either rAd-GFP-LC3B, derived from rat LC3 (GFP-M-LC3B, kindly provided by Sharon Tooze[10]), or rAd-EGFP-Av-LC3B. After 24 h, cells were infected with the nonpathogenic Beau-R[41] strain of IBV and 24 h postinfection cells were fixed and labeled with an anti-dsRNA antibody to detect the presence of IBV. As a control to confirm that these reagents could reproduce previous observations in mammalian cells, the experiment was also performed using Vero cells. As can be observed from **Figure 5A and B**, infection of Vero cells with IBV resulted in the induction of autophagic signaling and an increase number of puncta as demonstrated using both the mammalian and avian GFP-LC3B proteins. However, neither the mammalian nor the avian GFP-LC3B protein indicated the induction of autophagic signaling or an increase in number of puncta by IBV infection in either primary CK cells or DF1 cells, (**Fig. 5A, C and D**). Similar observations were made at 4, 8 and 16 h postinfection (hpi) with IBV (data not shown) and no dsRNA label could be detected in mock-infected cells (**Fig. 5G**). To determine whether this lack of induction of autophagic signaling in avian cells by IBV was related to virus pathogenicity, the experiment was repeated in CK cells using the pathogenic M41 strain of IBV. As can be seen from **Figure 5E and F**, infection by the pathogenic M41 strain also did not result in the induction of autophagic signaling or an increase in number of puncta in CK cells.

Infectious bronchitis virus Nsp6 induces autophagic signaling in avian cells. As previous work has shown that expression of the IBV replicase protein Nsp6 induces autophagy in Vero cells,[34] we wanted to determine whether expression of this protein alone is able to induce autophagic signaling in avian cells. DF1 cells were transfected with pmCherry-N1-nsp6 or

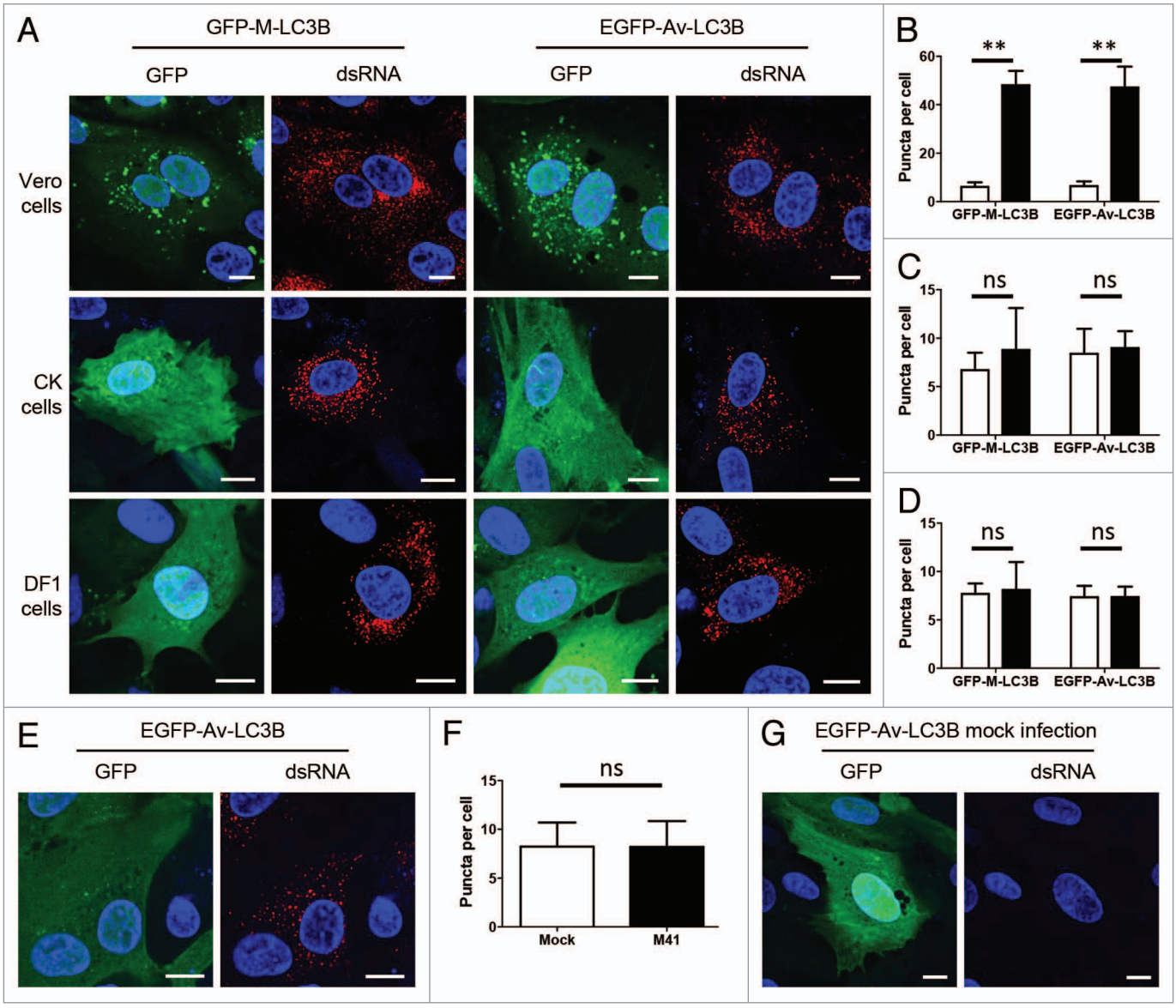

Figure 5. Infection of avian cells with IBV does not induce autophagic signaling. (**A**) Vero, CK and DF1 cells were transduced with rAd-GFP-M-LC3B (mammalian) or rAd-EGFP-Av-LC3B (avian) and after 24 h, cells were infected with IBV, Beau-R strain. At 24 hpi, cells were fixed and labeled with anti-dsRNA (red) to show IBV infection. Number of puncta per cell was determined in (**B**) Vero cells, (**C**) CK cells and (**D**) DF1 cells. Open bars, mock-infected cells; closed bars, IBV Beau-R infected cells. (**E**) CK cells were transduced with rAd-EGFP-Av-LC3B and after 24 h, cells were infected with M41 a pathogenic IBV strain. At 24 hpi, cells were fixed and labeled with anti-dsRNA (red). Nuclei (blue) are stained with DAPI. Scale bars: 10 μm. (**F**) Number of puncta per cell was determined from (**E**). Open bars, mock-infected cells; closed bars, IBV-infected cells. Mean plus standard deviation is shown for at least 20 cells from three independent experiments. **p ≤ 0.01 in a Student's t-test; ns, not significant in a Student's t-test. (**G**) Image of mock-infected cell from (**A**). CK cells were transduced with rAd-EGFP-Av-LC3B (green), mock-infected and labeled with anti-dsRNA (red). Nuclei (blue) are stained with DAPI. Scale bars: 10 μm.

pmCherry-N1-nsp10[34] and 24 h post transfection, transduced with rAd-GFP-Av-LC3B. After 24 h cells were fixed and examined using confocal fluorescence microscopy. As can be observed from **Figure 6A**, the EGFP-Av-LC3B protein has a predominantly diffuse distribution, comparable to untransfected cells, in DF1 cells expressing Nsp10-mCherry. However, EGFP-Av-LC3B showed a pronounced relocalization to cytoplasmic puncta when compared with untransfected cells, in DF1 cells expressing Nsp6-mCherry. In addition, there is a significantly higher number of puncta in cells expressing Nsp6 compared with Nsp10 (**Fig. 6B**). To confirm whether the puncta induced required post-translational modification of LC3 indicative of autophagosomes, cells were transfected with pmCherry-Nsp6 and transduced with recombinant adenovirus expressing EGFP-Av-LC3B G120A. Here, Nsp6 expression did not induce LC3 puncta (**Fig. 6C and D**). These results indicate that expression of the IBV Nsp6 replicase protein induced autophagic signaling in avian cells in a similar way as previously observed in Vero cells.[34]

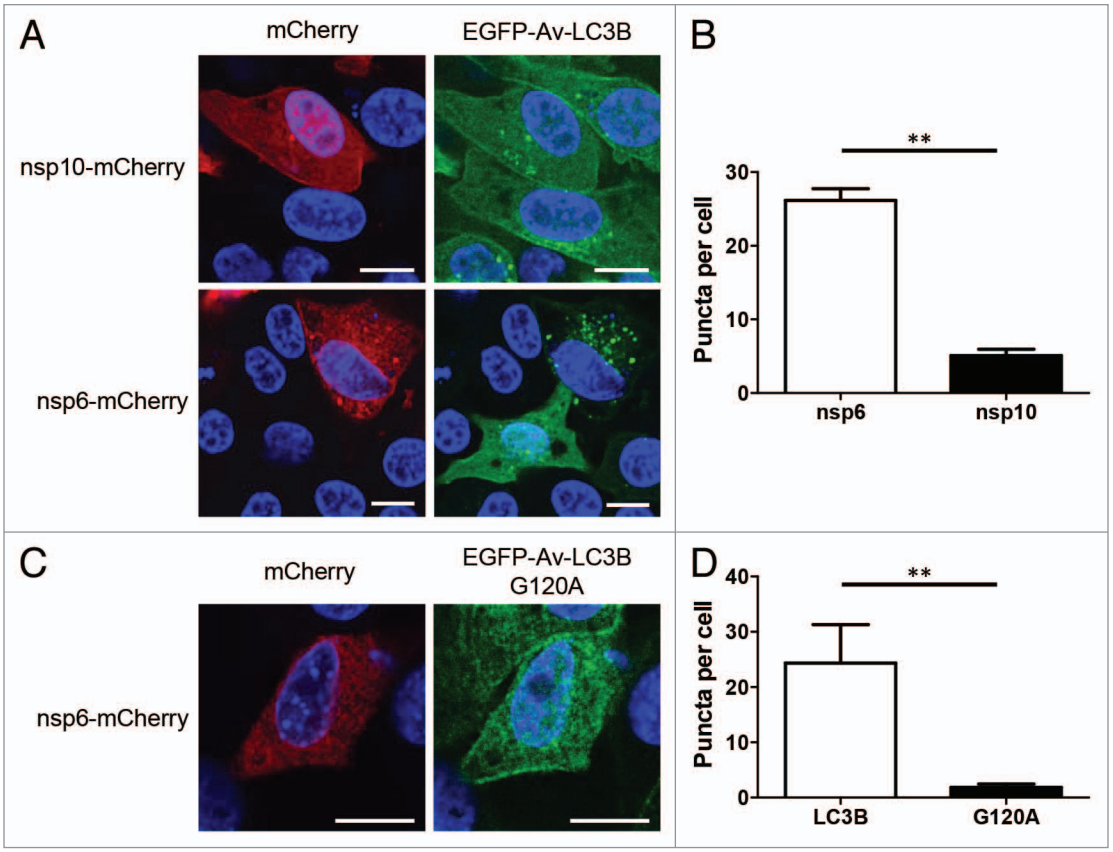

Figure 6. IBV replicase Nsp6 induces autophagic signaling in avian cells. (**A**) DF1 cells were transfected with pmCherry-N1-nsp6 or pmCherry-N1-nsp10 (red). After 24 h, cells were transduced with rAd-EGFP-Av-LC3B (green). Nuclei (blue) were stained with DAPI. Scale bars: 10 μm. (**B**) Number of puncta per cell was determined from (**A**) using Imaris spots software. (**C**) DF1 cells were transfected with pmCherry-N1-nsp6 (red) and after 24 h were transduced with rAd-EGFP-Av-LC3B G120A (green). Nuclei (blue) are stained with DAPI. Scale bars: 10 μm. (**D**) Number of puncta per cell was calculated from (**C**). Mean plus standard deviation is shown for at least 20 cells from three independent experiments. **p ≤ 0.01 in a Student's t-test.

Infectious bronchitis virus replication is not affected by autophagy induction or inhibition in avian cells. To determine whether autophagy plays a role during IBV replication in avian cells, CK cells were pretreated for 1 h in FM as a control, HBSS or rapamycin to induce autophagy or wortmannin to inhibit autophagy. Following treatment, CK cells were infected with Beau-R at a multiplicity of infection (MOI) of 10 or 0.1. Released progeny virus were harvested at 6 and 12 or 24 hpi, respectively, and titrated by plaque assay using CK cells. At 6 hpi, differences in virus titer between treatments were shown to be not significant by Student's t-test (**Fig. 7A**). At 12 and 24 hpi, induction of autophagy by starvation resulted in an approximately 10-fold reduction in virus titer (**Fig. 7B and C**). However, at 24 hpi there was a comparable reduction when cells were incubated in HBSS containing wortmannin (data sets were not significantly different by Student's t-test). When cells were incubated in FM containing either rapamycin to induce autophagy or wortmannin to inhibit autophagy, there was no change in virus titer. The effect of these treatments on LC3 lipidation was confirmed by western blot of endogenously expressed LC3 in CK cells (**Fig. 7D**). These observations suggest that IBV replication and subsequent release of progeny virus is affected by nutrient starvation but not by the induction or inhibition of autophagy.

Infectious bronchitis virus is not able to inhibit autophagy when induced by starvation or drug treatment. Several viruses have been identified that are able to inhibit induction of autophagy by inhibiting BECN1 or LC3 modification.[18,20,21] The observation that IBV infection does not induce autophagy in avian cells could be explained by the presence of an inhibitory signal in avian cells. To test this, CK cells were transduced to express EGFP-Av-LC3B, then mock-infected or infected with Beau-R and finally, at 24 hpi, the cells were incubated for 2 h in FM, as a control, or treated with HBSS or rapamycin to induce autophagy. Induction of autophagic signaling was determined by counting the number of puncta present per cell. As can be observed from **Figure 8** the mock-infected CK cells showed a significant increase in the number of puncta per cell when cells were starved (HBSS) or treated with rapamycin. However, when CK cells were infected with IBV and treated with FM, there was no increase in the number of puncta, indicating again that IBV does not induce autophagy in infected CK cells. Furthermore, when the IBV-infected CK cells were starved in HBSS or treated with rapamycin to induce autophagy, there was no decrease in the number of puncta when compared with the mock-infected CK cells. This observation indicates that IBV is not able to inhibit autophagy that has been induced by starvation in HBSS or by using rapamycin.

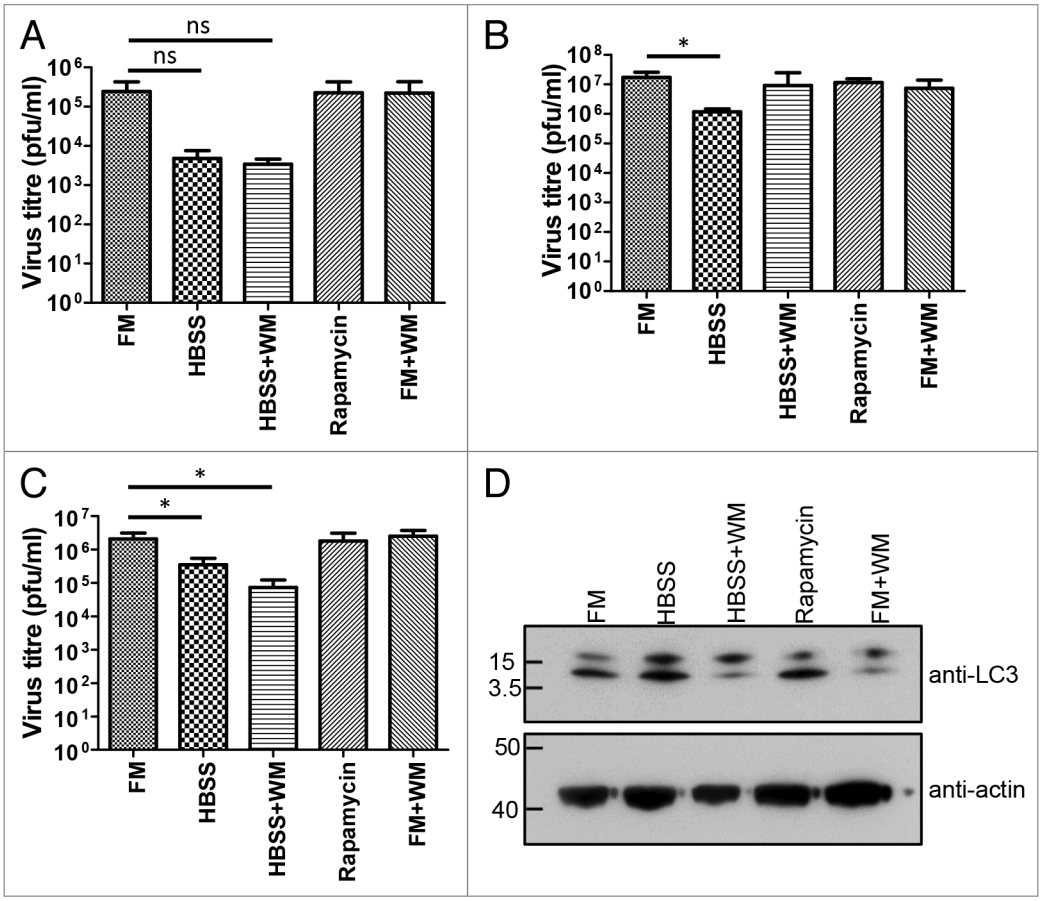

Figure 7. IBV replication is not affected by induction or inhibition of autophagy. CK cells were pretreated for 1 h in full medium (FM), Hank's balanced salt solution (HBSS), HBSS containing 10 nM wortmannin (HBSS+WM), FM containing 200 nM rapamycin (Rapamycin) or FM containing 10 nM wortmannin (FM+WM). Cells were then infected at (**A and B**) MOI 10 or (**C**) MOI 0.1 with IBV, Beau-R strain. At (**A**) 6 hpi, (**B**) 12 hpi or (**C**) 24 hpi, cell supernatant was harvested and titer of released progeny virus was assayed by plaque assay using CK cells. Bars show mean plus standard deviation for three independent experiments. *p = 0.05 in a Student's t-test; ns, not significant in a Student's t-test. (**D**) CK cells were washed and incubated for 1 h in FM, HBSS, HBSS+WM, Rapamycin or FM+WM. Cells were lysed and lysates separated on 10% NuPAGE in MOPS buffer. Proteins were detected by western blot with anti-LC3 or anti-actin.

Discussion

This is the first report of an avian reagent to study the generation of autophagosomes and their fusion with endosomes/lysosomes in avian cells. The reagents have been validated for use in studying the formation of autophagosomes in both primary and continuous avian cells (**Fig. 2**) and fusion of these labeled autophagosomes with endosomes/lysosomes (**Fig. 3**). Furthermore, although the mammalian homologs of LC3A and LC3C have been less frequently used to study autophagy, all three paralogs of avian LC3 were found to colocalize on the same structures upon cellular starvation (**Fig. 4**), despite differences in localization in uninduced cells where LC3C showed a reticular rather than diffuse localization (**Fig. 2**). This is in agreement with work performed by others demonstrating that rat derived GFP-LC3B colocalizes with human LC3A, LC3B and LC3C upon cellular starvation.[42] Furthermore, rat LC3A and two splice variants of LC3B were also shown to colocalize upon induction of autophagy, and the authors highlighted that all three proteins could be used as autophagosomal markers.[43] In addition, GABARAP and GABARAPL2/GATE-16, two other mammalian orthologs of yeast ATG8, have been shown to become conjugated to phosphatidylethanolamine (PE) and inserted into autophagosomal membranes[44] indicating that all ATG8 orthologs are likely to become inserted into the membranes of autophagosomes. A functional role for human LC3A variant 1 in autophagy has also been identified recently. Bai et al. have demonstrated that human LC3A variant 1, and not LC3B, is often inactivated in human tumor cell lines, as well as primary tumors, and a reduction in tumor growth can be achieved by restoring LC3A variant 1 expression.[45] These reports, as well as the variations in cellular localization observed here, highlight the differential role that the LC3 paralogs and isoforms may play in the various functions of autophagy.

The adenoviruses described here are particularly useful for transduction of primary avian cells, which are difficult to transfect with nonviral delivery systems based on cationic lipids. Importantly, these reagents will allow the study of the mechanism of autophagy in an avian system as well as the involvement of autophagy in economically important avian diseases. One

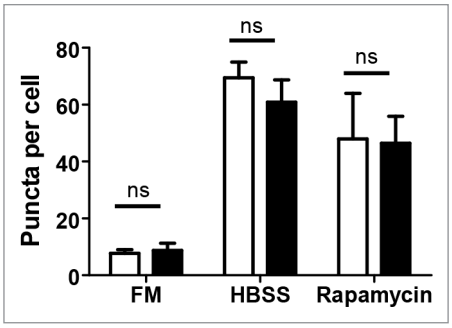

Figure 8. IBV does not inhibit autophagy induced by HBSS starvation or rapamycin. CK cells were transduced with rAd-EGFP-Av-LC3B and 24 h later, either mock-infected (open bars) or infected with IBV Beau-R (closed bars). At 24 hpi, cells were washed and incubated for a further 2 h in full medium (FM), Hank's balanced salt solution (HBSS) or FM containing 200 nM rapamycin (Rapamycin). Puncta per cell were determined using Imaris spots software. Bars show mean plus standard deviation for 20 cells counted from three independent experiments. ns, not significant in a Student's t-test.

such disease is infectious bronchitis, caused by the gammacoronavirus IBV. In our previous work, we demonstrated that infection of mammalian Vero cells with IBV resulted in the induction of autophagy at 24 hpi. Furthermore, when expressed individually, the membrane-bound IBV replicase protein Nsp6, but not Nsp4 or cytoplasmic Nsp10, induced autophagy. When analyzed further, this was shown to be via an omegasome intermediate and this characteristic was conserved for the Nsp6 homologs from other viruses within the *Nidovirales* order. Furthermore, Nsp6 induced autophagic flux because autophagosomes were demonstrated to fuse with lysosomes.[34] MHV, a betacoronavirus, has also been shown to induce autophagy in infected cells.[31] Furthermore, both SARS-CoV and MHV have been described to induce double-membrane vesicles (DMVs) upon infection of cells[29,30] and recently, we have also identified DMVs in primary CK cells infected with IBV (Maier et al. in preparation). Historically, it has been assumed that these DMVs provide a platform for the assembly of viral replication complexes. As DMVs resemble cellular autophagosomes in structure, a role for autophagy in the generation of DMVs has often been suggested.

In this study we have confirmed that IBV induces autophagic signaling in Vero cells. However, this does not appear to be the case in avian cells, both primary and a continuous cell line (**Fig. 5A–D**). Furthermore, this phenotype was not affected by the degree of virus pathogenicity as a known pathogenic IBV isolate was also shown to be deficient in autophagic signaling induction (**Fig. 5E and F**). In addition, our work demonstrated that IBV replication does not appear to be altered by either induction or inhibition of autophagy (**Fig. 7**). Starvation of cells with HBSS did result in a modest 10-fold reduction of viable progeny virus at 12 and 24 hpi. However, when autophagy was inhibited with wortmannin in the presence of HBSS at 24 hpi, there was no recovery of virus titer. This suggests that the lack of nutrients may result in a reduction of the ability of the cell to support the high burden of virus replication. An alternative reason could be that the released progeny virus is unstable in HBSS. Importantly, when cells were treated in full medium containing either rapamycin or wortmannin, there was no significant difference in the levels of progeny virus. This is in agreement with our previous work where *ATG5* knockdown by siRNA does not affect IBV infection in Vero cells.[34] It is also consistent with reports that MHV replication is not affected by siRNA knockdown of *ATG5*[32] or *ATG7*.[33] Together, these data indicate that classical autophagy does not play a major role in the replication cycle of IBV or other coronaviruses. Knoops et al. have demonstrated by electron tomography that DMVs observed in SARS-CoV-infected cells actually form part of a complex network of membranes, linked via the outer membrane to each other and to the ER and therefore, DMVs resemble autophagosomes less than previously thought.[29] In this case, a role for autophagy in the development of DMVs seems less likely. Furthermore, another report has demonstrated that DMVs formed during MHV infection are closely linked to the EDEMosome pathway and not autophagy, with LC3-I rather than LC3-II playing an important role.[33]

In contrast to the observations during virus infection, when expressed alone, IBV Nsp6 was shown to induce autophagic signaling in an avian cell line in a process requiring LC3 post-translational cleavage and lipidation (**Fig. 6**), presumably via an analogous route to that observed in mammalian cells.[34] Previous observations show that IBV Nsp6 and homologs from other members of the *Nidovirales* order, MHV and porcine respiratory and reproductive syndrome virus (PRRSV), induce autophagy but do not enter autophagosomes. However, the Nsp6 protein from SARS-CoV does partially colocalize with LC3, indicating that Nsp6 is incorporated into autophagosomes.[34] Interestingly, here we observed that some IBV Nsp6 did enter autophagosomes as there was a degree of colocalization with avian GFP-LC3B, although this was more evident in some cells than others. This again highlights a difference in protein function when expressed in mammalian and avian cells. One explanation for the discrepancy between results observed for virus infection and expression of Nsp6 individually is that perhaps any signal from Nsp6 to induce autophagic signaling is masked when the protein is assembled into the virus replication complex. As one of only three coronavirus membrane-bound Nsps, Nsp6, with Nsp3 and Nsp4, is thought to provide an anchor for the large replication complex, tethering it to the membrane. In this complex, the host cell may no longer be able to detect the stimulatory signals. If replication complex assembly is less efficient in mammalian cells than in avian cells due to differences in host cofactors, free Nsp6 may exist in mammalian cells, which is then detected by the cell as an activating signal for autophagy. Alternatively, IBV may encode a mechanism to inhibit autophagy during infection that is functional in avian cells but not in mammalian cells. If autophagy is not playing an active role in virus replication, it may be playing a role in innate cellular defense to the virus. However, when tested, IBV was not capable of suppressing autophagy when induced by starvation or rapamycin treatment (**Fig. 8**), although we cannot rule out that IBV can inhibit autophagy at an upstream step of these signals or via an alternative route of autophagy signaling. Presumably, IBV would inhibit autophagy by inhibiting the signaling pathway that is activated by Nsp6. Interestingly, Nsp6

has been previously shown not to induce autophagy via MTOR inactivation in Vero cells, or via ER stress or sirtuin 1 signaling and the mechanism of induction of autophagy remains unidentified.[34] Therefore, identification of this mechanism would allow further investigation of any possible inhibitory signals encoded by IBV.

Materials and Methods

Cells, antibodies and reagents. Primary chick kidney (CK) cells were produced from 1–3 week-old chickens hatched from specific pathogen free (SPF) eggs and primary chick embryo fibroblast (CEF) cells were produced from 9 d-old embryonated SPF eggs of the Rhode Island Red line of domesticated chickens held at the IAH. DF1 cells, a continuous cell line derived from chicken embryonic fibroblasts,[46] were used as a representative avian cell line. Monoclonal anti-LAMP1 antibody[37] (formally LEP100), developed by Douglas M. Fambrough, was obtained from the Developmental Studies Hybridoma Bank developed under the auspices of the NICHD and maintained by the University of Iowa, Department of Biology, Iowa City, IA 52242. Monoclonal J2 anti-dsRNA was purchased from English and Scientific Consulting Bt. (10010200). Goat anti-mouse IgG (H^+L)-Alexa 568 was purchased from Invitrogen (A11004). Construction of pmCherry-N1-nsp6 and pmCherry-N1-nsp10 has been described previously.[34]

Cloning of the avian LC3 genes. The avian orthologs of the mammalian *LC3A* (XM_417327 and XP_417327), *LB3B* (NM_001031461 and NP_001026632) and *LC3C* (XM_419549 and XP_419549) precursor genes were identified in the genome of the Red Junglefowl (*Gallus gallus*), using the Ensembl database. Oligonucleotides were designed from the avian *LC3A*, *LC3B* and *LC3C* transcript sequences (**Table 1**) and were used to generate copies of the *Gallus gallus domesticus LC3A*, *LB3B* and *LC3C* transcripts from cellular RNA extracted from CK cells using TRIzol (Invitrogen, 15596-026). The cDNAs of the three avian *LC3* paralogs were generated using reverse transcription PCR (RT-PCR). Briefly, reverse transcription was performed using SuperScript II (Invitrogen, 18064022) for *LC3A* or Superscript III (Invitrogen, 18080093) for *LC3B* and *LC3C* according to the manufacturer's instructions. PCR was performed, according to the manufacturer's instructions, using Expand Taq High Fidelity (Roche, 04738250001) for *LC3A* using the following cycle; step 1, 94°C 2 min, step 2, 94°C 15 sec, 65°C 30 sec, 72°C 1 min, step 3, 72°C 7 min, step 4, 4°C hold with step 2 repeated to give 35 cycles or Phusion high fidelity DNA polymerase (Finnzymes, F-530L) for *LC3B* and *LC3C* using the following cycle; step 1, 98°C 30 sec, step 2, 98°C 10 sec, 55°C or 65°C 45 sec, 72°C 1 min, step 3, 72°C 2 min, step 4, 4°C hold with step 2 repeated to give 30 cycles. The avian-derived *LC3* cDNAs were initially inserted into pmCherry-C1 (Clontech, 632524) between the *XhoI* and *BamHI* restriction endonuclease sites to generate N-terminally mCherry-tagged versions of the three avian *LC3* paralogs, mCherry-Av-*LC3A*, mCherry-Av-*LC3B* and mCherry-Av-*LC3C* in plasmids pmCherry-C1-Av-*LC3A*, pmCherry-C1-Av-*LC3B* and pmCherry-C1-Av-*LC3C*. Sequence analysis of the RT-PCR generated *Gallus gallus domesticus LC3* paralogs confirmed that they were the same as the reported Red Junglefowl LC3 sequences at the amino acid level. The avian *LC3*s were subcloned into pEGFP-C1 (Clontech, 6084-1) between the *XhoI* and *BamHI* sites, to generate N-terminally GFP tagged versions of the three avian LC3 paralogs, EGFP-Av-*LC3A*, EGFP-Av-*LC3B* and EGFP-Av-*LC3C*, in plasmids pEGFP-C1-Av-*LC3A*, pEGFP-C1-Av-*LC3B* and pEGFP-C1-Av-*LC3C*.

Expression of avian EGFP-LC3 and FLAG-mCherry-LC3 by recombinant adenoviruses. The N-terminally EGFP-tagged avian *LC3* genes were PCR amplified from plasmids pEGFP-C1-Av-*LC3A*, *-LC3B* and *-LC3C* (**Table 1**), initially inserted into pENTR/D-TOPO (Invitrogen, K240020) and finally subcloned into pAd/CMV/V5-DEST (Invitrogen, V49320) using LR clonase (Invitrogen, 11791100), according to the manufacturer's instructions. The N-terminally FLAG-mCherry tagged avian *LC3* genes were generated by PCR amplification from pmCherry-C1-Av-*LC3A*, pmCherry-C1-Av-*LC3B* and pmCherry-C1-Av-*LC3C* using a forward primer encoding a FLAG tag at the 5' end (**Table 1**). The products were cloned into pENTR/D-TOPO and subcloned into pAd/CMV/V5-DEST, as before. The EGFP-tagged avian *LC3B* G120A construct was generated by PCR mutagenesis using pENTR/D-TOPO-EGFP-Av-*LC3B* as a template and primers containing the desired mutation (**Table 1**). Replication-defective recombinant human adenoviruses (Ad5), rAd5-EGFP-Av-LC3A, rAd5-EGFP-Av-LC3B, rAd5-EGFP-Av-LC3C, rAd-FLAG-mCherry-Av-LC3A, rAd-FLAG-mCherry-Av-LC3B, rAd-FLAG-mCherry-Av-LC3C and rAd5-EGFP-Av-LC3B G120A were rescued using the ViraPower protocol (Invitrogen). Briefly, 293 cells were transfected with each pAd/CMV/V5-DEST construct, previously linearized using *Pac*I, and cultured in complete medium (DMEM, 10% FCS) until cytopathic effect (CPE) was observed by microscopy. The cells were harvested and lysed by freeze/thaw to release the virus particles. This cell lysate was used to infect a bulk preparation of 293 cells and the culture harvested when CPE was evident throughout the cell monolayer. The resultant recombinant adenovirus was partially purified using discontinuous CsCl gradient ultracentrifugation, in which 6 ml of virus supernatant was overlaid on a cushion of 3.5 ml of 1.25 g/ml CsCl (1.98 M CsCl in 10 mM Tris pH 7.8) and 3.5 ml of 1.35 g/ml CsCl (2.78 M CsCl in 10 mM Tris pH 7.8) and centrifuged using a Beckman Coulter SW40 Ti rotor (Beckman Coulter, Inc.) or Sorvall Th-641 rotor (Thermo Fisher Scientific) for 2 h at 80,000 × g in a Beckman Coulter Optima L-80 XP ultra centrifuge (Beckman Coulter, Inc.) or Sorvall WX Ultra 80 ultra centrifuge (Thermo Fisher Scientific). Following centrifugation the lower band, containing intact virus, was removed and further purified using isopycnic CsCl gradient ultracentrifugation, in which 7 ml of the partially purified virus supernatant was overlaid on 6 ml of 1.35 g/ml CsCl and centrifuged using a Beckman Coulter SW40 Ti rotor or Sorvall Th-641 rotor for 18 h at 115,000 × g in a Beckman Coulter Optima L-80 XP ultra centrifuge or Sorvall WX Ultra 80 ultra centrifuge. Again the lower band containing purified intact virus was removed and dialysed against storage buffer (10 mM Tris, 7.5% w/v sucrose, pH 7.8). Recombinant viruses

Table 1. Sequence of primers used to clone avian LC3 paralogs and generate recombinant adenovirus vectors

Primer Name	Sequence 5' → 3'
***LC3A* F**	CCG **CTC GAG** CTA CCA TGC CCT CGG ACC GGG CCT TC
***LC3A* R**	GTC G**GG ATC C**CG GTA GCC AAA GGT CTC CTG
***LC3B* F**	ATC G**CT CGA G**CT ACC ATG CCC TCG GAG AAG AGC TTC
***LC3B* R**	ATC G**GG ATC C***CT A*GA CGG AAG ATT GCA CTC C
***LC3C* F**	ATC G**CT CGA G**CT ACC ATG CAG GCG GGT CCC GGG GTG
***LC3C* R**	ATC G**GG ATC C***CT A*GG TTT TAT GAT GGC ATT C
EGFP F	CAC CAT GGT GAG CAA GGG CGA GGA GCT GTT CAC C
FLAG mCherry F	CAC CAT GGA TTA TAA GGA TGA CGA TGA CAA AGT GAG CAA GGG CGA GGA GGA TAA CAT GGC C
TOPO-*LC3A* R	*TCA* GTA GCC AAA GGT CTC CTG GGA AGC GTA
TOPO-*LC3B* R	*CTA* GAC GGA AGA TTG CAC TCC GAA AGT CTC
TOPO-*LC3C* R	*CTA* GGT TTT ATG ATG GCA TTC CAT AGT TTT C
***LC3B* G120A F**	AGG AGA CTT TCG *CT*G TGC AAT CTT CC
***LC3B* G120A R**	GGA AGA TTG CAC *AG*C GAA AGT CTC CT

Inserted restriction sites are highlighted in bold, stop codons are italicised, the FLAG tag is underlined and mutated bases are italicized and underlined. LC3 sequences were taken from the codon immediately after the ATG start codon. The avian *LC3* nucleotide sequence accession numbers used were *LC3A* XM_417327.2, *LC3B* NM_001031461 and *LC3C* XM_419549.

Table 2. Pearson's correlation coefficient for colocalization of EGFP-Av-LC3 with LAMP1

EGFP-Av-LC3A	0.57 (± 0.08)
EGFP-Av-LC3B	0.51 (± 0.17)
EGFP-Av-LC3C	0.64 (± 0.02)

Mean plus standard deviation shown from three independent experiments.

were titrated to determine the amount required to produce 75% or more GFP or mCherry expressing CK, CEF or DF1 cells at 24 h post-transduction.[10]

Confocal microscopy. CK, CEF or DF1 cells were seeded onto glass coverslips in 24 well plates. Cells were transduced with recombinant adenovirus and incubated at 37°C for 24 h. Cells were then washed 4 times using Hank's balanced salt solution (HBSS, Sigma, H8264) and treated for 2 h at 37°C to induce or inhibit autophagy. Control cells were incubated in full-nutrient media (FM). Cells were starved by incubation in HBSS to induce autophagy or were incubated in 10 nM wortmannin in HBSS to inhibit autophagy. Following these treatments, cells were fixed for 20 min in 4% paraformaldehyde, nuclei stained with 4',6-diamidino-2-phenylindole (DAPI) and the coverslips were mounted onto glass slides. For studying endosomal/lysosomal fusion, cells were washed four times using HBSS and then starved in HBSS. After 2 h incubation at 37°C, cells were fixed at –20°C in ice-cold methanol for 4 min, blocked for 15 min using 2% BSA in phosphate-buffered saline (PBS), incubated with monoclonal anti-LAMP1 at a dilution of 1:1000 in 2% BSA in PBS and washed three times using 2% BSA in PBS. Cells were then incubated with secondary antibody anti-mouse-Alexa 568 (Invitrogen, A11004) diluted 1:200 in 2% BSA in PBS, washed three times using 2% BSA in PBS, stained with DAPI and the coverslips mounted onto glass slides. For studying autophagy in IBV infected cells, at 24 h post rAd transduction cells were washed 4 times using PBS and then infected with IBV, either the apathogenic Beau-R[41] or pathogenic M41 strain. Twenty-four hours postinfection with IBV, cells were either fixed immediately using 4% paraformaldehyde or washed four times and incubated for 2 h in FM, HBSS or FM containing 200 nM rapamycin (Sigma, R0395) to induce autophagy. Cells were fixed for 20 min in 4% paraformaldehyde, permeabilized for 15 min using 0.1% triton X-100 in PBS and blocked for 1 h in 0.5% BSA in PBS. Virus infection was detected using monoclonal anti-dsRNA J2 in 0.5% BSA in PBS at a dilution of 1:1000 followed by secondary antibody anti-mouse-Alexa 568 diluted 1:200 in 0.5% BSA in PBS. Coverslips were analyzed using a Leica DM6000 confocal microscope using LAS AF software (version 2.6.0.7266, Leica Microsystems CMS GmbH). Spot counts were performed on at least 20 cells using spot module in Imaris 7.6 software (Bitplane Scientific Software). Colocalization analysis was performed using the coloc module of Imaris software using the polygon model. Data displayed is percent material colocalized in region of interest and Pearson's correlation coefficient in region of interest.

Transfection of DF1 cells. DF1 cells were seeded onto glass coverslips in 24-well plates. Cells were washed once with PBS and incubated in 500 µl fresh medium. Transfection complexes were set up in 10 µl OptiMEM (Invitrogen, 51985-026) by addition of 0.3 µg plasmid and 0.75 µl FugeneHD (Promega, E2311). After 15 min incubation at room temperature, the transfection mix was added to the cells. After 6 h, cells were washed and 500 µl fresh medium added and after an additional 18 h the cells were transduced with recombinant adenovirus and analyzed as described above.

Western blot. DF1 cells were transduced with recombinant adenovirus and after 24 h, were washed 4 times using HBSS. Cells were then incubated for 1 h in full-nutrient media, HBSS or HBSS containing 10 nM wortmannin. CK cells were washed 4 times in HBSS and incubated for 1 h in full-nutrient media, HBSS, HBSS containing 10 nM wortmannin, full-nutrient

Table 3. Pearson's correlation coefficient for colocalization of EGFP-Av-LC3 with FLAG-mCherry-Av-LC3

	FLAG-mCherry-Av-LC3A	FLAG-mCherry-Av-LC3B	FLAG-mCherry-Av-LC3C
EGFP-Av-LC3A	0.70 (± 0.05)	0.63 (± 0.03)	0.68 (± 0.09)
EGFP-Av-LC3B	0.67 (± 0.01)	0.53 (± 0.05)	0.63 (± 0.07)
EGFP-Av-LC3C	0.61 (± 0.03)	0.68 (± 0.04)	0.65 (± 0.04)

Mean plus standard deviation shown from three independent experiments.

media containing 200 nM rapamycin or full-nutrient media containing 10 nM wortmannin. Cells were washed in cold PBS and lysed in RIPA buffer [150 mM sodium chloride, 50 mM TRIS-HCl pH 7.4, 1% Igepal, 0.25% Sodium deoxycholate, 1 mM ethylene glycol tetraacetic acid, 1 mM phenylmethylsulfonyl fluoride, 1 mM sodium orthovanadate, 1 mM sodium fluoride and 1x protease inhibitor cocktail (Sigma Aldrich, P8340)]. Cell lysates were separated on a 10% NuPAGE gel (Invitrogen, NP0302BOX) in MOPS buffer (Invitrogen, NP0001). Proteins were transferred to PVDF membrane (Gilson Scientific, Ltd., PV4HY00010) and incubated in 0.5% MARVEL milk powder in PBS containing 0.1% TWEEN-20. Proteins were detected using anti-GFP diluted at 1:1000 (Abcam, ab290), anti-LC3 diluted at 1:1000 (Sigma Aldrich, L7543) or anti-actin diluted at 1:750 (actin α, β and λ, Abcam, ab3280). For Nsp6 experiments, DF1 cells were washed once with PBS and incubated in 3 ml fresh DMEM containing 10% FCS. Transfection complexes were set up in 100 μl OptiMEM by addition of 2 μg plasmid and 8 μl FugeneHD. After 15 min incubation, the transfection mix was added to the cells. After 6 h, cells were washed and 3 ml fresh media added. After a further 16 h, cells were transduced with recombinant adenovirus and treated as described. Cell lysates were processed and analyzed as described above.

IBV replication. CK cells were pretreated for 1 h in FM, HBSS, HBSS containing 10 nM wortmannin, FM containing 200 nM rapamycin or FM containing 10 nM wortmannin. Cells were then infected with IBV Beau-R strain at MOI 10 or 0.1, continuing in the same treatment as listed above. After 6 and 12 or 24 h, respectively, cell supernatant was harvested and assayed for released progeny virus by plaque assay.

Disclosure of Potential Conflicts of Interest

No potential conflicts of interest were disclosed.

Acknowledgments

This work was supported by the Biotechnology and Biological Sciences Research Council (BBSRC) grant BB/E01805X/1 to PB and BB/E018521/1 to TW and two Society for General Microbiology vacation studentships awarded to Helena Maier, Christopher Harte and Jessica Wilkinson. The authors would like to thank Sharon Tooze for providing recombinant adenoviruses and for useful discussions, Ali Turner, Jake Matthews and the Viral Vector Core facility, University of Oxford, for assistance with adenovirus amplification and purification and Pete Kaiser and Mark Gibson for identification of the *Gallus gallus LC3* genes.

References

1. Ding WX, Yin XM. Sorting, recognition and activation of the misfolded protein degradation pathways through macroautophagy and the proteasome. Autophagy 2008; 4:141-50; PMID:17986870
2. Kapahi P, Chen D, Rogers AN, Katewa SD, Li PWL, Thomas EL, et al. With TOR, less is more: a key role for the conserved nutrient-sensing TOR pathway in aging. Cell Metab 2010; 11:453-65; PMID:20519118; http://dx.doi.org/10.1016/j.cmet.2010.05.001
3. Levine B. Eating oneself and uninvited guests: autophagy-related pathways in cellular defense. Cell 2005; 120:159-62; PMID:15680321; http://dx.doi.org/10.1016/S0092-8674(05)00043-7
4. Levine B, Klionsky DJ. Development by self-digestion: molecular mechanisms and biological functions of autophagy. Dev Cell 2004; 6:463-77; PMID:15068787; http://dx.doi.org/10.1016/S1534-5807(04)00099-1
5. Yoshimori T. Autophagy: a regulated bulk degradation process inside cells. Biochem Biophys Res Commun 2004; 313:453-8; PMID:14684184; http://dx.doi.org/10.1016/j.bbrc.2003.07.023
6. Lang T, Schaeffeler E, Bernreuther D, Bredschneider M, Wolf DH, Thumm M. Aut2p and Aut7p, two novel microtubule-associated proteins are essential for delivery of autophagic vesicles to the vacuole. EMBO J 1998; 17:3597-607; PMID:9649430; http://dx.doi.org/10.1093/emboj/17.13.3597
7. Suzuki K, Kirisako T, Kamada Y, Mizushima N, Noda T, Ohsumi Y. The pre-autophagosomal structure organized by concerted functions of APG genes is essential for autophagosome formation. EMBO J 2001; 20:5971-81; PMID:11689437; http://dx.doi.org/10.1093/emboj/20.21.5971
8. Kabeya Y, Mizushima N, Ueno T, Yamamoto A, Kirisako T, Noda T, et al. LC3, a mammalian homologue of yeast Apg8p, is localized in autophagosome membranes after processing. EMBO J 2000; 19:5720-8; PMID:11060023; http://dx.doi.org/10.1093/emboj/19.21.5720
9. Mizushima N, Yamamoto A, Matsui M, Yoshimori T, Ohsumi Y. In vivo analysis of autophagy in response to nutrient starvation using transgenic mice expressing a fluorescent autophagosome marker. Mol Biol Cell 2004; 15:1101-11; PMID:14699058; http://dx.doi.org/10.1091/mbc.E03-09-0704
10. Köchl R, Hu XW, Chan EY, Tooze SA. Microtubules facilitate autophagosome formation and fusion of autophagosomes with endosomes. Traffic 2006; 7:129-45; PMID:16420522; http://dx.doi.org/10.1111/j.1600-0854.2005.00368.x
11. Strecker V, Mai S, Muster B, Beneke S, Bürkle A, Bereiter-Hahn J, et al. Aging of different avian cultured cells: lack of ROS-induced damage and quality control mechanisms. Mech Ageing Dev 2010; 131:48-59; PMID:19948180; http://dx.doi.org/10.1016/j.mad.2009.11.005
12. Mizushima N, Yamamoto A, Hatano M, Kobayashi Y, Kabeya Y, Suzuki K, et al. Dissection of autophagosome formation using Apg5-deficient mouse embryonic stem cells. J Cell Biol 2001; 152:657-68; PMID:11266458; http://dx.doi.org/10.1083/jcb.152.4.657
13. Tooze SA, Razi M. The essential role of early endosomes in autophagy is revealed by loss of COPI function. Autophagy 2009; 5:874-5; PMID:19502778.
14. Kudchodkar SB, Levine B. Viruses and autophagy. Rev Med Virol 2009; 19:359-78; PMID:19750559; http://dx.doi.org/10.1002/rmv.630
15. Wileman T. Aggresomes and autophagy generate sites for virus replication. Science 2006; 312:875-8; PMID:16690857; http://dx.doi.org/10.1126/science.1126766
16. Cottam E, Pierini R, Roberts R, Wileman T. Origins of membrane vesicles generated during replication of positive-strand RNA viruses. Future Virology 2009; 4:473-85; http://dx.doi.org/10.2217/fvl.09.26
17. Liang XH, Kleeman LK, Jiang HH, Gordon G, Goldman JE, Berry G, et al. Protection against fatal Sindbis virus encephalitis by beclin, a novel Bcl-2-interacting protein. J Virol 1998; 72:8586-96; PMID:9765397
18. Orvedahl A, Alexander D, Tallóczy Z, Sun Q, Wei Y, Zhang W, et al. HSV-1 ICP34.5 confers neurovirulence by targeting the Beclin 1 autophagy protein. Cell Host Microbe 2007; 1:23-35; PMID:18005679; http://dx.doi.org/10.1016/j.chom.2006.12.001
19. Shelly S, Lukinova N, Bambina S, Berman A, Cherry S. Autophagy is an essential component of Drosophila immunity against vesicular stomatitis virus. Immunity 2009; 30:588-98; PMID:19362021; http://dx.doi.org/10.1016/j.immuni.2009.02.009
20. Ku B, Woo JS, Liang C, Lee KH, Hong HS, e X, et al. Structural and biochemical bases for the inhibition of autophagy and apoptosis by viral BCL-2 of murine gamma-herpesvirus 68. PLoS Pathog 2008; 4:e25; PMID:18248095; http://dx.doi.org/10.1371/journal.ppat.0040025
21. Sinha S, Colbert CL, Becker N, Wei Y, Levine B. Molecular basis of the regulation of Beclin 1-dependent autophagy by the gamma-herpesvirus 68 Bcl-2 homolog M11. Autophagy 2008; 4:989-97; PMID:18797192

22. Zhou Z, Jiang X, Liu D, Fan Z, Hu X, Yan J, et al. Autophagy is involved in influenza A virus replication. Autophagy 2009; 5:321-8; PMID:19066474; http://dx.doi.org/10.4161/auto.5.3.7406
23. Gannagé M, Dormann D, Albrecht R, Dengjel J, Torossi T, Rämer PC, et al. Matrix protein 2 of influenza A virus blocks autophagosome fusion with lysosomes. Cell Host Microbe 2009; 6:367-80; PMID:19837376; http://dx.doi.org/10.1016/j.chom.2009.09.005
24. Grégoire IP, Richetta C, Meyniel-Schicklin L, Borel S, Pradezynski F, Diaz O, et al. IRGM is a common target of RNA viruses that subvert the autophagy network. PLoS Pathog 2011; 7:e1002422; PMID:22174682; http://dx.doi.org/10.1371/journal.ppat.1002422
25. Sun Y, Li C, Shu Y, Ju X, Zou Z, Wang H, et al. Inhibition of autophagy ameliorates acute lung injury caused by avian influenza A H5N1 infection. Sci Signal 2012; 5:ra16; PMID:22355189; http://dx.doi.org/10.1126/scisignal.2001931
26. Kyei GB, Dinkins C, Davis AS, Roberts E, Singh SB, Dong C, et al. Autophagy pathway intersects with HIV-1 biosynthesis and regulates viral yields in macrophages. J Cell Biol 2009; 186:255-68; PMID:19635843; http://dx.doi.org/10.1083/jcb.200903070
27. Panyasrivanit M, Khakpoor A, Wikan N, Smith DR. Co-localization of constituents of the dengue virus translation and replication machinery with amphisomes. J Gen Virol 2009; 90:448-56; PMID:19141455; http://dx.doi.org/10.1099/vir.0.005355-0
28. Jackson WT, Giddings TH Jr., Taylor MP, Mulinyawe S, Rabinovitch M, Kopito RR, et al. Subversion of cellular autophagosomal machinery by RNA viruses. PLoS Biol 2005; 3:e156; PMID:15884975; http://dx.doi.org/10.1371/journal.pbio.0030156
29. Knoops K, Kikkert M, Worm SH, Zevenhoven-Dobbe JC, van der Meer Y, Koster AJ, et al. SARS-coronavirus replication is supported by a reticulovesicular network of modified endoplasmic reticulum. PLoS Biol 2008; 6:e226; PMID:18798692; http://dx.doi.org/10.1371/journal.pbio.0060226
30. Ulasli M, Verheije MH, de Haan CAM, Reggiori F. Qualitative and quantitative ultrastructural analysis of the membrane rearrangements induced by coronavirus. Cell Microbiol 2010; 12:844-61; PMID:20088951; http://dx.doi.org/10.1111/j.1462-5822.2010.01437.x
31. Prentice E, Jerome WG, Yoshimori T, Mizushima N, Denison MR. Coronavirus replication complex formation utilizes components of cellular autophagy. J Biol Chem 2004; 279:10136-41; PMID:14699140; http://dx.doi.org/10.1074/jbc.M306124200
32. Zhao Z, Thackray LB, Miller BC, Lynn TM, Becker MM, Ward E, et al. Coronavirus replication does not require the autophagy gene ATG5. Autophagy 2007; 3:581-5; PMID:17700057
33. Reggiori F, Monastyrska I, Verheije MH, Calì T, Ulasli M, Bianchi S, et al. Coronaviruses Hijack the LC3-I-positive EDEMosomes, ER-derived vesicles exporting short-lived ERAD regulators, for replication. Cell Host Microbe 2010; 7:500-8; PMID:20542253; http://dx.doi.org/10.1016/j.chom.2010.05.013
34. Cottam EM, Maier HJ, Manifava M, Vaux LC, Chandra-Schoenfelder P, Gerner W, et al. Coronavirus nsp6 proteins generate autophagosomes from the endoplasmic reticulum via an omegasome intermediate. Autophagy 2011; 7:1335-47; PMID:21799305; http://dx.doi.org/10.4161/auto.7.11.16642
35. Larkin MA, Blackshields G, Brown NP, Chenna R, McGettigan PA, McWilliam H, et al. Clustal W and Clustal X version 2.0. Bioinformatics 2007; 23:2947-8; PMID:17846036; http://dx.doi.org/10.1093/bioinformatics/btm404
36. Tamura K, Dudley J, Nei M, Kumar S. MEGA4: Molecular Evolutionary Genetics Analysis (MEGA) software version 4.0. Mol Biol Evol 2007; 24:1596-9; PMID:17488738; http://dx.doi.org/10.1093/molbev/msm092
37. Lippincott-Schwartz J, Fambrough DM. Lysosomal membrane dynamics: structure and interorganellar movement of a major lysosomal membrane glycoprotein. J Cell Biol 1986; 102:1593-605; PMID:2871029; http://dx.doi.org/10.1083/jcb.102.5.1593
38. Chen Q, Fang L, Wang D, Wang S, Li P, Li M, et al. Induction of autophagy enhances porcine reproductive and respiratory syndrome virus replication. Virus Res 2012; 163:650-5; PMID:22119900; http://dx.doi.org/10.1016/j.virusres.2011.11.008
39. Lee YR, Lei HY, Liu MT, Wang JR, Chen SH, Jiang-Shieh YF, et al. Autophagic machinery activated by dengue virus enhances virus replication. Virology 2008; 374:240-8; PMID:18353420; http://dx.doi.org/10.1016/j.virol.2008.02.016
40. Wong J, Zhang J, Si X, Gao G, Mao I, McManus BM, et al. Autophagosome supports coxsackievirus B3 replication in host cells. J Virol 2008; 82:9143-53; PMID:18596087; http://dx.doi.org/10.1128/JVI.00641-08
41. Casais R, Thiel V, Siddell SG, Cavanagh D, Britton P. Reverse genetics system for the avian coronavirus infectious bronchitis virus. J Virol 2001; 75:12359-69; PMID:11711626; http://dx.doi.org/10.1128/JVI.75.24.12359-12369.2001
42. He H, Dang Y, Dai F, Guo Z, Wu J, She X, et al. Post-translational modifications of three members of the human MAP1LC3 family and detection of a novel type of modification for MAP1LC3B. J Biol Chem 2003; 278:29278-87; PMID:12740394; http://dx.doi.org/10.1074/jbc.M303800200
43. Wu J, Dang Y, Su W, Liu C, Ma H, Shan Y, et al. Molecular cloning and characterization of rat LC3A and LC3B--two novel markers of autophagosome. Biochem Biophys Res Commun 2006; 339:437-42; PMID:16300744; http://dx.doi.org/10.1016/j.bbrc.2005.10.211
44. Kabeya Y, Mizushima N, Yamamoto A, Oshitani-Okamoto S, Ohsumi Y, Yoshimori T. LC3, GABARAP and GATE16 localize to autophagosomal membrane depending on form-II formation. J Cell Sci 2004; 117:2805-12; PMID:15169837; http://dx.doi.org/10.1242/jcs.01131
45. Bai H, Inoue J, Kawano T, Inazawa J. A transcriptional variant of the LC3A gene is involved in autophagy and frequently inactivated in human cancers. Oncogene 2012; 31:4397-408; PMID:22249245; http://dx.doi.org/10.1038/onc.2011.613
46. Himly M, Foster DN, Bottoli I, Iacovoni JS, Vogt PK. The DF-1 chicken fibroblast cell line: transformation induced by diverse oncogenes and cell death resulting from infection by avian leukosis viruses. Virology 1998; 248:295-304; PMID:9721238; http://dx.doi.org/10.1006/viro.1998.9290